FAILURE CHARACTERIZATION OF LAMINATION EPOXY UTILIZING 3D DIGITAL IMAGE CORRELATION UNDER DIFFERENT LOADING CONDITIONS

Elruby, A.[1]*, and Nakhla, S.[2]
[1] Assistant Professor, Mechanical Engineering, Memorial University, St. John's, Canada
[2] Associate Professor, Mechanical Engineering, Emergency Medicine, Memorial University, St. John's, Canada
* Corresponding author (aelruby@mun.ca)

Keywords*: Failure, Lamination Epoxy, 3D DIC*

ABSTRACT

Composite structures are widely used in various engineering applications such as aerospace, ship and automotive industries. Composite structures are usually preferred over conventional metals for their superior mechanical properties and stiffness-to-weight ratios. However, composite materials' failure modes are complex due to the different failure mechanisms of their constituents and their bonding. Two of the four typical failure modes of composites are dominated by the resin (matrix) material. The current work aims at precisely characterizing the mechanical behavior of lamination epoxy used in aerospace applications. In addition, investigating the failure mechanisms utilizing high precision non-contact 3D digital image correlation (DIC) for strain measurements. Also, post-failure fractographic investigations are provided utilizing scan electron microscopy (SEM). The manufacturer provided the plain epoxy which was machined to the desired specimens' geometry at Memorial University's facilities. The same patch was used to prepare two sets of specimens for testing under uniaxial loading and three-point bending. The specimens were prepared as per the ASTM standards, namely, ASTM D638 and ASTM D790 for the tensile and the three-point bending, respectively. A total of five specimens were prepared for each test. The specimens were tested in an electrical load frame (Instron 5585H). Two high-speed cameras were used for DIC together with a GOM high-precision panel for calibration. Post-failure analysis was conducted on fractured specimens to identify the failure mechanisms. Scan electron microscopy (SEM) was employed for this purpose. Initial results of the current investigations show damage initiation locations and enabled identifying the failure mechanisms.

1 INTRODUCTION

Composite structures are commonly used in numerous engineering applications such as aerospace, automotive, and ship industries. The main advantage over conventional engineering materials is their high stiffness-to-weight ratios [1]. However, composites exhibit complex failure mechanisms whether related to their individual constituents' failure limits or the chemical bonding and adhesion between these constituents, i.e., the fibers and the resin [2], [3]. The resin material dominates two out of four failure modes, namely, matrix cracking and delamination [4], [5]. The resin is subject to mainly shear stresses and its failure is dominated by combined loading scenarios [6]. Characterizing the failure mechanisms of plain epoxy under different types of loading scenarios is of a chief importance in composite industry and various engineering applications.

In the current work, plain lamination epoxy is provided by the manufacturer for thorough characterization. Two sets of specimens are prepared for testing under different loading conditions, namely, uniaxial and three-point bending. Fractographic analyses are provided to better investigate the damage process and identify the associated failure mechanisms.

2 Material and Specimen Preparation

2.1 Material

Lamination epoxy resin used in aerospace applications was provided by the manufacturer, i.e., Polynt Composites Canada, Inc., for the purpose of the current work. Characterizing the plain epoxy resin would enable better understanding of the associated failure mechanisms which is the main goal of the proposed work. The epoxy system was manufactured by using a 6:1 resin to hardener weight ratio and cured in a mold. The physical properties as provided by the manufacturer are provided in Table 1.

Table 1. Lamination epoxy physical properties at room temperature

Material/Property	Viscosity (mPs)	Density (g/ml)	Weight (%)	Shelf life (days)	Pot life (minutes)	Tack free (minutes)
Resin EPO-LP61	~1300	~1.10	85.72	90	~25	~300
Hardener EP-OLC61	~35	~0.97	14.28			

2.2 Specimen Preparation

The provided epoxy slab was used to prepare two sets of specimens for mechanical characterization under different loading conditions. The first set consisted of a total of 5 specimens which exceeds the minimum number specified by the ASTM D638 testing standard [7]. The flat specimens were machined down to a thickness of 5mm from the original slab thickness to ensure flawless surfaces from both sides. Type I specimen geometry was followed from the ASTM designation and a schematic diagram outlining the major dimensions is shown in Figure 1.

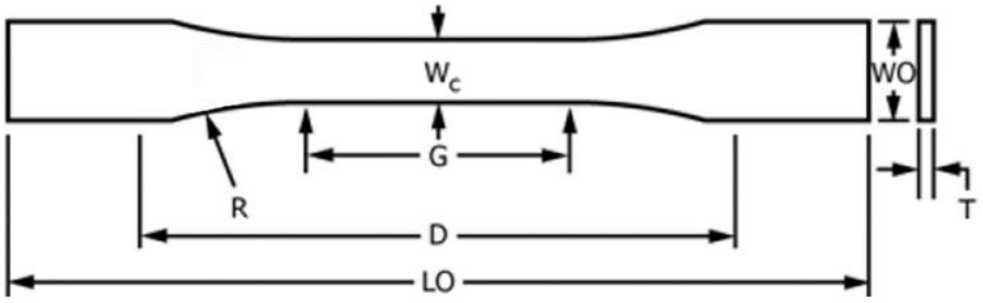

Wc	13 mm
WO	19 mm
LO	165 mm
G	50 mm
D	115 mm
R	76 mm
T	5 mm

Figure 1. Flat tensile specimen geometry and major dimensions, adapted from [7]

The second set of specimens was machined as per ASTM D790 designation [8] to characterize the flexural properties of the lamination epoxy resin. Five prismatic specimens were machined from the same batch used for the flat tensile specimens. The prisms were made of a rectangular cross-section, namely, $12.7\ mm \times 6.8\ mm$ and a total span of $127\ mm$ as shown in Figure 2.

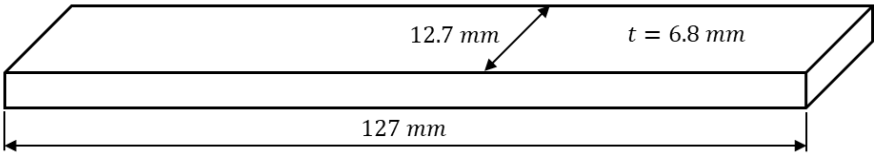

Figure 2. Prismatic specimen geometry as per ASTM D790, i.e., geometry is not drawn to scale

3 Test Setup

3.1 Load Frame and 3D DIC System

An electromechanical load frame was utilized for all the mechanical characterization, namely, the E5585H Instron load frame with a maximum capacity of $250\ kN$. A non-contact high precision relative deformation measurement was enabled by relying on a stereo system for imaging. The system consisted of two high-speed cameras, namely, model Megaspeed MS130K. Two $40\ mm$ Nikon lenses were used to enable focusing on the speckled specimens for digital image correlation. Employing a stereo system, i.e., two cameras enables three-dimensional (3D) measurements. The load frame and the stereo system are presented in Figure 3.

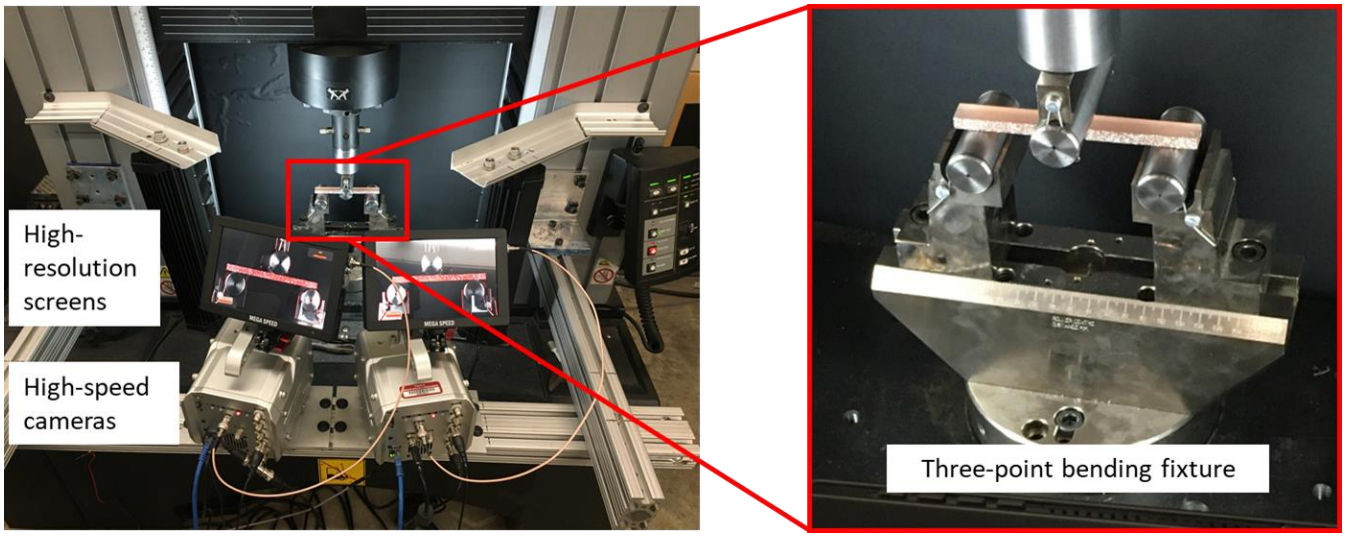

Figure 3. E5585 Instron load frame utilized with a high-speed stereo system for imaging and digital image correlation.

Speckling the specimens is an essential step for digital image correlation. A sharp contrast should be achieved by spraying layers of black and white paint successively. During the speckle preparation, it was observed that this method is not suitable for the epoxy specimens which have an opaque transparent color. Utilizing a black background as shown in Figure 3 and only white paint to speckle the specimen alleviated this challenge and resulted in an excellent focus on the stochastic patterns prior to testing. Those stochastic patterns are the ones identified by

the digital image correlation (DIC) software for strain measurements. They are simply blocks of pixels that can be identified prior to deformation and during testing, these same blocks are tracked. GOM Correlate Professional 2017 software was utilized in analyzing all the measurements. The stereo system was calibrated for 3D DIC using a standard GOM coded Panel ($MV\ 55 \times 44\ mm^2$). These standard panels are manufactured with a 1µm precision to enable precise measurements upon calibrating the system. The calibration resulted in a measurement volume equal to $155 \times 90 \times 70\ mm$ with a calibration deviation equal to 0.032 pixels, i.e., less than one-third of a micron.

4 Testing Results

4.1 Tensile Tests

All the tested specimens showed a linear type behavior followed by a sudden failure owed to the brittleness nature of glassy polymers such as epoxy. Glassy polymers are known to exhibit this type of behavior under uniaxial loading conditions. The main purpose of this test is to characterize the mechanical properties such as the modulus of elasticity, Poisson's ratio and the failure limits, i.e., failure stress and strain. The reported engineering stress-strain behavior from testing is presented in Figure 4. As can be observed that the specimens almost showed same mechanical behavior with the exception of slight variations towards their failure limits.

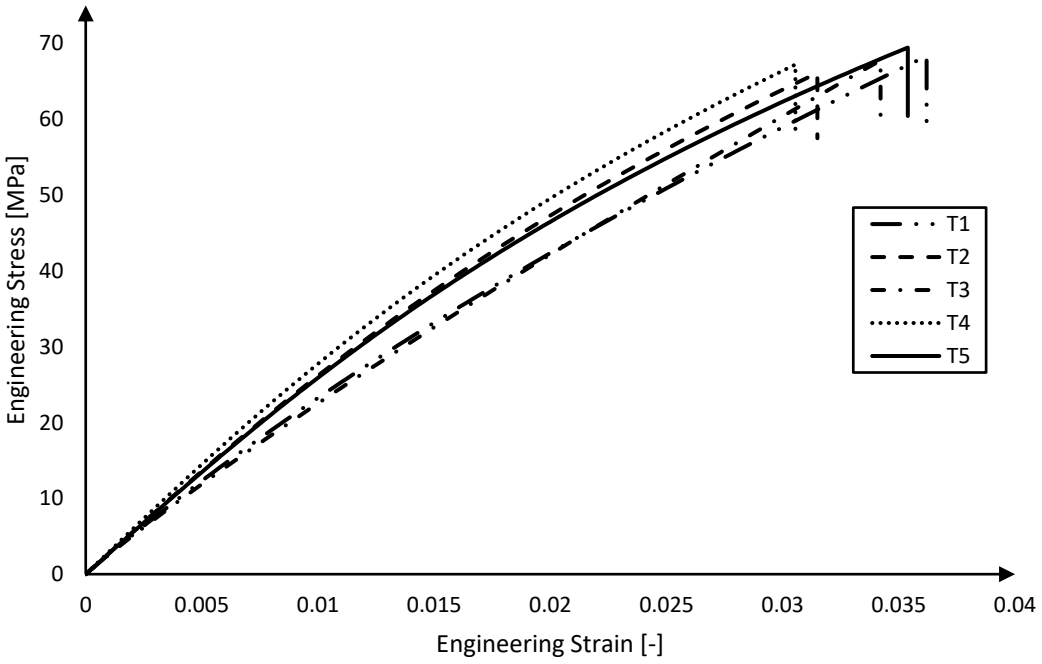

Figure 4. Engineering stress-strain results of tensile testing

The details of the mechanical properties are documented in Table 2. The lowest and the highest moduli of elasticity were reported for specimens T1 and T4, respectively. The highest and the lowest failure stresses were recorded by specimens T5 and T2, respectively. Finally, the extrema of the failure strains were reported by specimens T1 and T4.

Table 2. Tensile test mechanical properties and failure limits.

Specimen number	Modulus of Elasticity (GPa)	Failure Stress (MPa)	Failure Strain (%)
T1	2.36	68.32	3.62
T2	2.67	66.08	3.15
T3	2.28	67.76	3.42
T4	2.85	67.20	3.05
T5	2.64	69.44	3.54

Full-field strain measurements from DIC analysis using GOM Correlate Professional are depicted at different time frames in Figure 5. Each figure is showing the strain field individually and superimposed on the specimen T5 during the test. The last time frame was a few seconds before the final failure. Noteworthy to mention, that an extra step of validating the DIC measurements was performed by attaching a physical extensometer to the gauge length of the specimen. A virtual extensometer was utilized in the software to match the physical one. Both results were compared and they were identical.

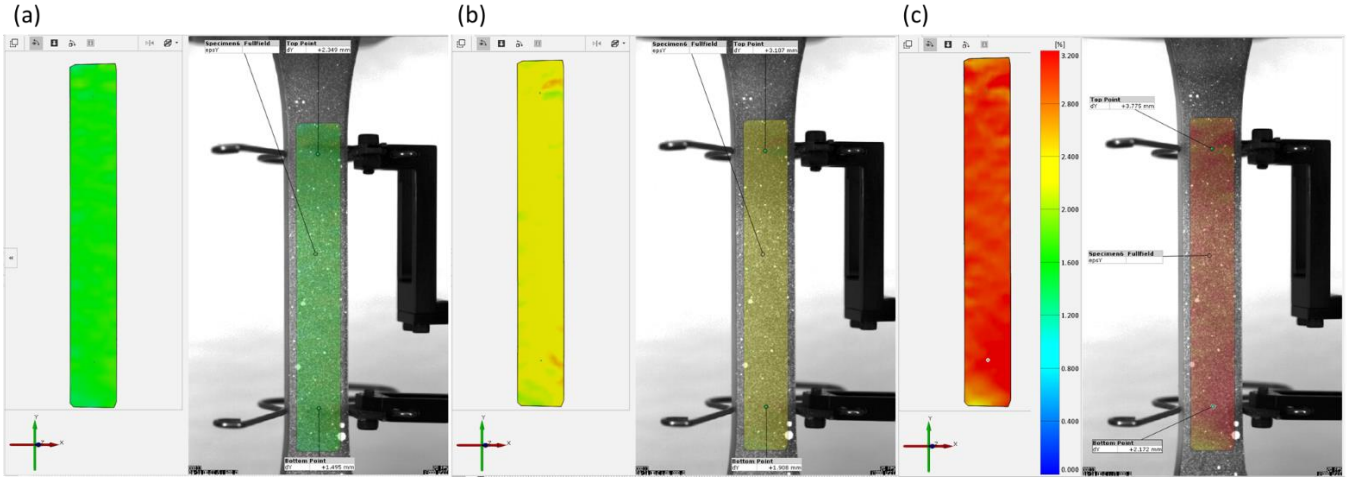

Figure 5. Full-field strain measurements along the longitudinal direction from the DIC analysis at different time frames: (a) 51 sec (b) 66 sec (c) 77 sec

4.2 Three-Point Bending Tests

All the tested specimens showed almost identical behavior despite the fact that their failure loads and deflections varied. The behavior of lamination epoxy under combined loading conditions, i.e., three-point bending, showed larger variations in terms of failure limits. Specimens P2 and P3 were the ones reporting the extrema limits, namely, the lowest and the highest failure limits, respectively. Also, the variation between these extrema is significant were it went above 25% for the failure load and above 35% for the failure deflection. The detailed values of the corresponding failure limits are documented in Table 3 while the reported flexural load-deflection curves are presented in Figure 6.

Table 3. Flexural failure limits of three-point bending tests

Specimen	P1	P2	P3	P4	P5
Failure Load (N)	404	371	464	430	452
Failure Deflection (mm)	8.333	7.708	10.483	9.271	9.792

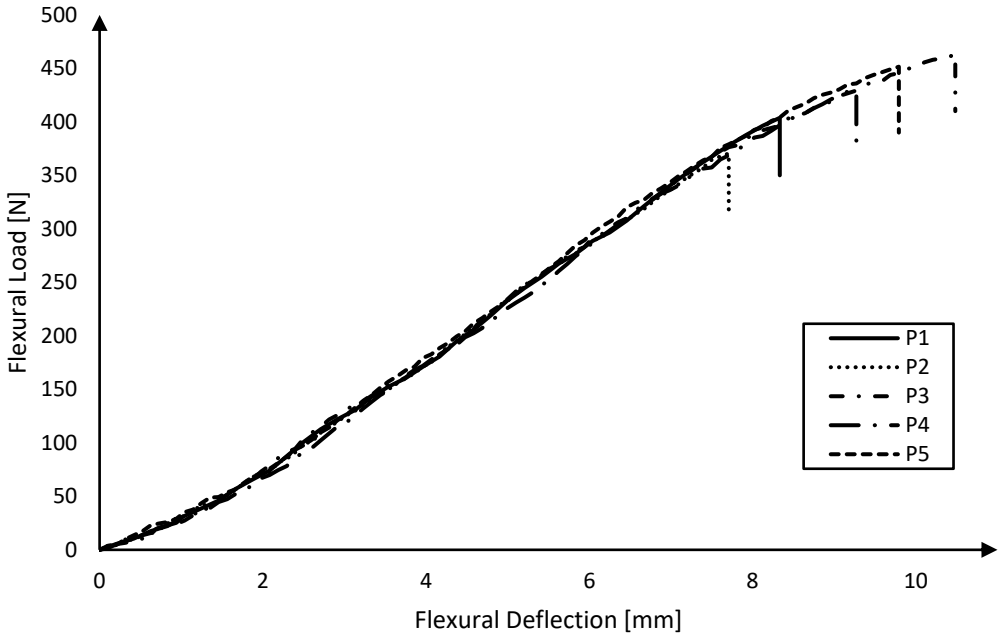

Figure 6. Flexural load-deflection results of the three-point bending tests

The full-field strain measurements of specimen P4 at different time frames are presented in Figure 7. The full-field strain measurements clearly identify the tension and compressive strains on the prism during loading. As the load increased the top roller became in the way of the sensor, i.e., HS cameras, which caused the loss of some regions in the strain field measurements as can be observed in Figure 7(a) Figure 7(b). However, the remaining regions still provided insight into the mechanical behavior.

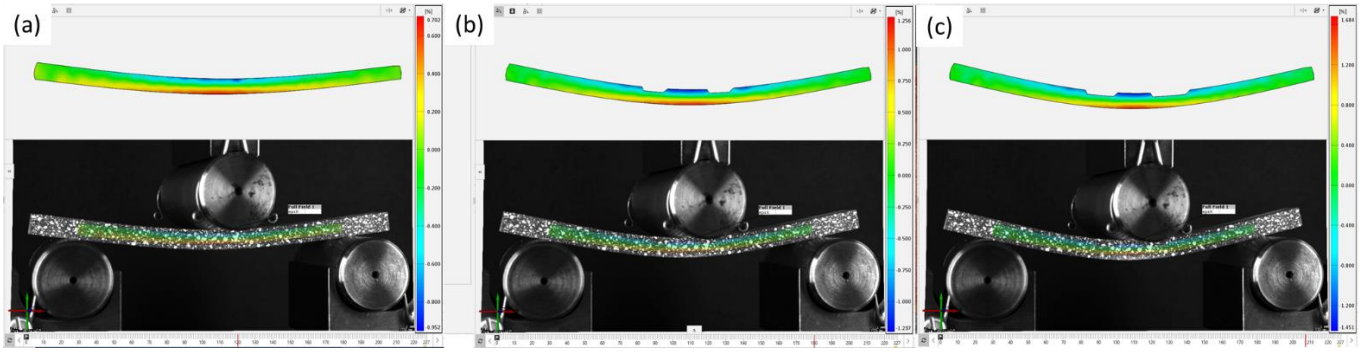

Figure 7. Full-field strain measurements along the longitudinal direction from the DIC analysis at different time frames: (a) 120 sec (b) 180 sec (c) 207 sec

5 Post-Failure Analysis

5.1 Tensile Specimens Fractured Surfaces

In this section, the fractured surfaces from both tests were investigated. A closer observation of micro-length scales will indeed enable a better understanding of the failure mechanisms associated with different loading conditions. The lamination epoxy under uniaxial loading exhibited brittle failure dominated by normal stresses. In fact, this was evident from the fractured surfaces being normal to the load application direction. On top of that, examining the fractured surface utilizing scan electron microscopy (SEM) revealed an interesting observation regarding the damage initiation process at micro-length scales. For example, specimen T2 fractured surface was investigated using SEM as shown in Figure 8. It can be observed from Figure 8(a) that the locus of the damage process was in the vicinity of the center of this specimen. A scatter of crazes or cracking originating from a small void can be observed from the zoomed-in view as presented in Figure 8(b). This indicates that the damage process of the lamination epoxy was triggered at a micro-length scale due to the presence of a stress raiser, i.e., micro-void. The presence of micro-voids in epoxies is unavoidable owing to their chemical polymerization process. This process is an exothermic process where these micro-voids tend to form in the mix prior to solidification.

Another example from the tensile specimens showed that the damage process was initiated by a surface flaw. This is also common for brittle or quasi-brittle materials such as polymeric materials, i.e. lamination epoxy in the current work. Figure 9 shows the fractured surface of specimen T4 as an example of such behavior. On the right-hand side of Figure 9(a) the edge of the specimen is showing the origin of the damage process. A zoomed-in view is provided in Figure 9(b) for better illustration. The nature of the surface micro-flaw is not distinguished. It cannot be confirmed whether this flaw was a void or just a micro-scratch on the surface.

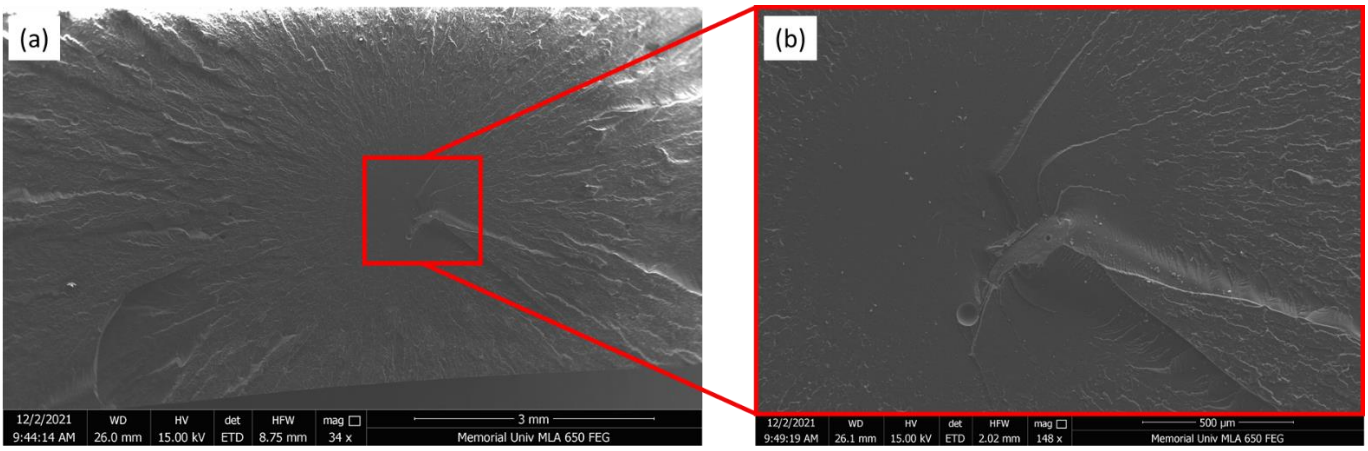

Figure 8. Specimen T2 fractured surface investigation using scan electron microscopy (a) lower magnification (b) higher magnification

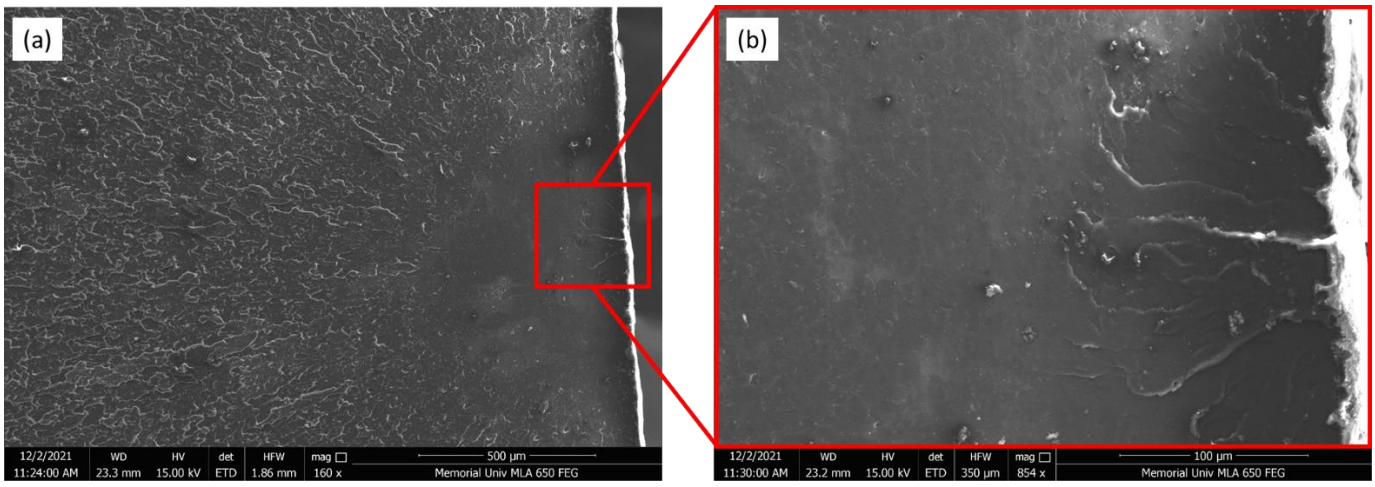

Figure 9. Specimen T4 fractured surface investigation using scan electron microscopy (a) lower magnification (b) higher magnification

5.2 Three-Point Bending Specimens Fractured Surfaces

A prism under a three-point bending load exhibits maximum normal and shear stress at mid-span. This combined loading scenario would be closer to practically applied loads. Also, the material would exhibit going through the prism depth from tension to compression. In addition, the matrix material in a composite is mainly carrying shear stress alongside the normal ones. This load combination resulted in mixed-mode failures that were observed in all the tested specimens. Figure 10(a) shows the fractured surface of specimen P2 where two distinct failure modes can be observed. On the left-hand side, an unstable failure is associated with small chip pieces that chattered upon final failure while the right-hand side shows a flat surface signifying that normal stresses dominated this failure. Moreover, there exists a locus for the damage initiation which can be better observed from the zoomed-in view presented in Figure 10(b). In fact this is very similar to the mechanisms observed in the tensile specimens.

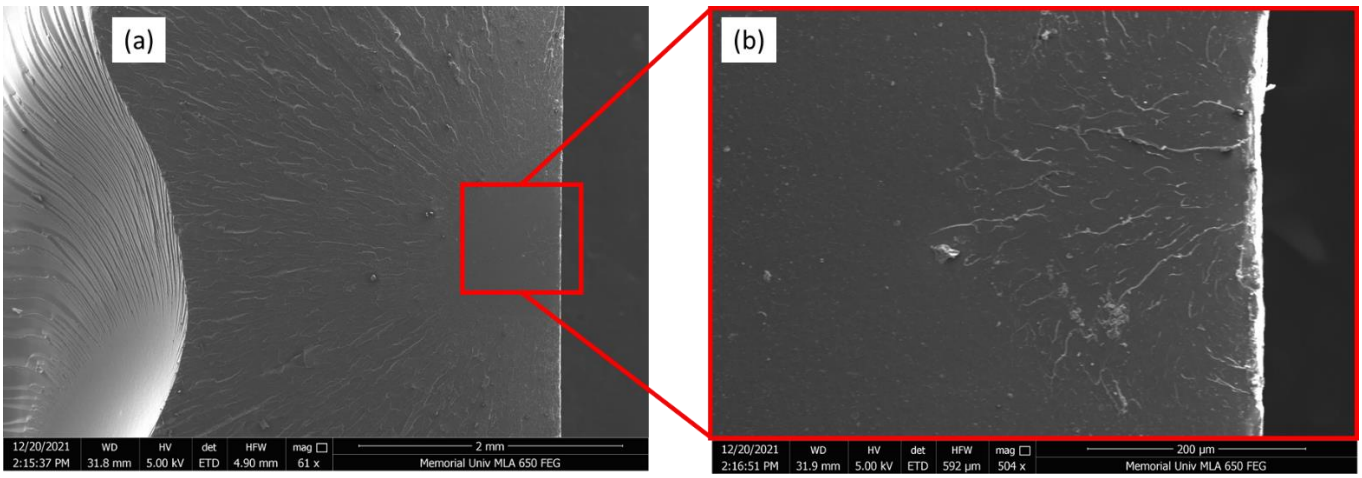

Figure 10. Specimen P2 fractured surface investigation using scan electron microscopy (a) lower magnification (b) higher magnification

A second example is provided by the fracture surface of specimen P5 as presented in Figure 11. This fracture surface shows that the failure initiated in the tension side of the prism, i.e., the left-hand side of the Figure 11(a). The locus

of the micro-damage process is located towards the surface center which then propagated in a radial manner towards the other side of the prism. Figure 11(b) shows a zoomed-in view on a transition region of changing failure mechanisms.

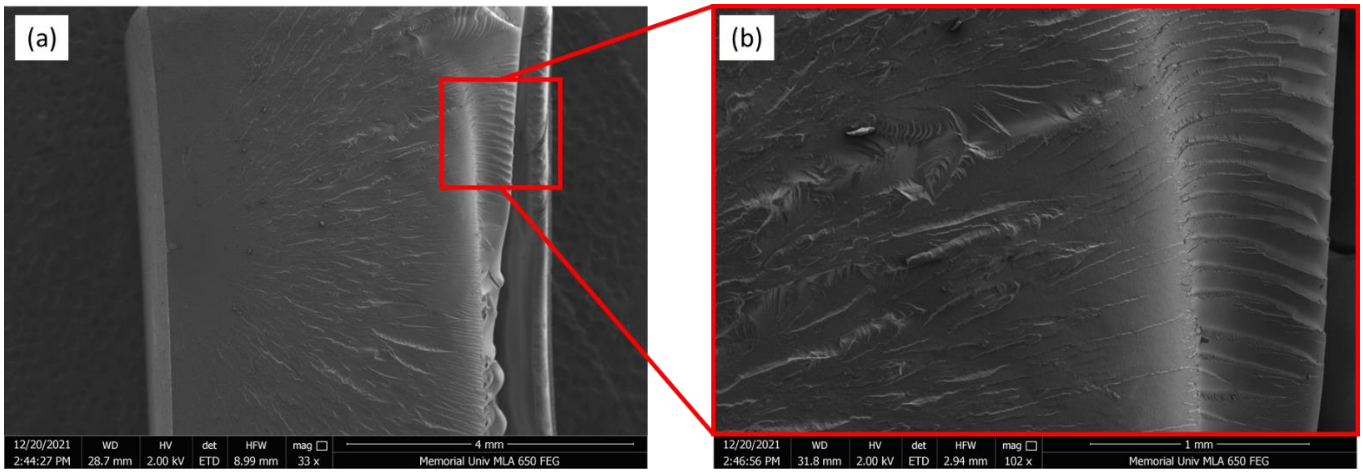

Figure 11. Specimen P5 fractured surface investigation using scan electron microscopy (a) lower magnification (b) higher magnification

6 Conclusions and Future Work

Lamination epoxy was tested under different loading conditions, namely, uniaxial loading and three-point bending. The main objective of the current work was to thoroughly characterize the mechanical behavior of lamination epoxy under different loading conditions. Two sets of specimens were machined according to the associated ASTM standards. The specimens were tested in an electromechanical load frame utilizing high-precision digital image correlation for strain measurements. The mechanical characterization properties for the lamination epoxy were documented and presented in the current work. Also, fractographic analyses we performed to better investigate different failure mechanisms. Scan electron microscopy was employed for that purpose which revealed multiple microscopic features and better identified the associated the damage process initiation. It can be concluded that lamination epoxy exhibits a quasi-brittle behavior when loaded under uniaxial tensile loads. A combined loading scenario closer to practical loading conditions cause mixed-mode failures. These failure were evident to merge from one type to another. The authors suggest a further investigation on analytical models to predict failure under combined loads.

7 REFERENCES

[1] P.K. Mallick, *Fiber-Reinforced Composites: Materials, Manufacturing, and Design*. 2007.

[2] H. Koerber *et al.*, “Experimental characterization and constitutive modeling of the non-linear stress–strain behavior of unidirectional carbon–epoxy under high strain rate loading,” *Adv. Model. Simul. Eng. Sci.*, 2018.

[3] A. Elruby, S. Handrigan, and S. Nakhla, “Fracture Behavior of Heavily Cross-linked Epoxy; Testing, Fractography and Numerical Modeling,” *Eng. Mater. Technol.*, 2020.

[4] J. Bieniaś, H. Dębski, B. Surowska, and T. Sadowski, “Analysis of microstructure damage in carbon/epoxy composites using FEM,” *Comput. Mater. Sci.*, vol. 64, pp. 168–172, 2012.

[5] Y. Yang, X. Liu, Y. Q. Wang, H. Gao, R. Li, and Y. Bao, “A progressive damage model for predicting damage evolution of laminated composites subjected to three-point bending,” *Compos. Sci. Technol.*, vol. 151, pp. 85–93, 2017.

[6] A. Y. Elruby and S. Nakhla, “Strain energy density based damage initiation in heavily cross-linked epoxy using XFEM,” *Theor. Appl. Fract. Mech.*, vol. 103, no. May, p. 102254, 2019.

[7] ASTM D638, “Standard test method for tensile properties of plastics,” *ASTM Int.*, vol. 08, pp. 46–58, 2015.

[8] ASTM-D790-17, “Standard Test Methods for Flexural Properties of Unreinforced and Reinforced Plastics and Electrical Insulating Materials,” *ASTM Int. Des. D*, pp. 1–12, 2017.